

Quantitative Measurement of Electric Fields in Microelectronics Devices by *In-Situ* Pixelated STEM

Victor Boureau¹, Lucas Bruas², Matthew Bryan², Jean-Luc Rouvière³ and David Cooper^{2*}

¹. Interdisciplinary Center for Electron Microscopy, EPFL, Lausanne, Switzerland.

². Univ. Grenoble Alpes, CEA, Leti, Grenoble, France.

³. Univ. Grenoble Alpes, CEA, IRIG-MEM, Grenoble, France.

* Corresponding author: david.cooper@cea.fr

The quantitative mapping of fields at nanometer scale is essential to understand the behavior of devices and improve their performance. Historically this has been performed by off-axis electron holography, as this technique is mature and provides robust quantitative measurements [1]. In recent years, improvements in hardware have made possible the recording of diffraction patterns during a scanning transmission electron microscopy (STEM) experiment, generating so-called 4D-STEM datasets. An increasing number of data processing methods, combined with specific acquisition settings, have led to a wide range of pixelated STEM techniques [2]. Here, we explore the differential phase contrast (DPC) technique [3], performed in a pixelated STEM configuration [4]. It allows for the quantitative measurement of electric fields based on the intensity displacements of the transmitted beam in the diffraction plane. We will show how DPC-like pixelated STEM measurements are affected by the configuration of the microscope and by data processing. The results will be compared to electron holography and simulations.

To begin, we will present work on a silicon *p-n* junction doped with a symmetrical 10^{19} cm^{-3} concentration, examined at a reverse bias of -1.3 V. Using this specimen there are no changes in mean inner potential (composition) and the bias voltage increases the built-in electric field. A cross-section of the junction was prepared by focused ion beam and attached to a chip for *in-situ* biasing experiments using a Protochips Aduro 500 sample holder in a FEI Titan microscope operated at 200 kV. The specimen is shown in Figs. 1(a,b) and has a crystalline thickness of 390 nm, as measured by convergent beam electron diffraction. The electric field in the junction was modeled with Silvaco software using secondary ion mass spectrometry dopant measurement as an input. The profile across the junction is shown in Fig. 1(c). The electric field of the biased junction was measured by off-axis electron holography, see Figs. 1(c,d), and shows a good agreement with the modeling after the inactive thickness has been removed [1]. The electric field of the reverse-biased *p-n* junction has a magnitude of about 0.65 MV.cm^{-1} and a depletion width of about 60 nm.

Different pixelated STEM configurations and processing methods have been investigated for the measurement of the electric field in the junction. When the probe size was larger than the characteristic field variation length leading to a redistribution of intensity inside the transmitted beam, a center-of-mass (CoM) algorithm was used. When the transmitted beam was smaller than the field variation and undergoes a rigid-shift, a template matching (TM) algorithm was used [5]. Firstly, a low-magnification (LM) STEM configuration was used, using a half convergence angle of 270 μrad and a camera length of 18 m. The diffraction pattern in the junction shows a redistribution of intensity at the edges of the transmitted beam so CoM processing is used, see Fig. 2(a). The electric field map is shown in Fig. 2(e) and a profile is plotted in Fig. 2(i). The depletion width of the junction appears to be about 100 nm, which demonstrates a loss of spatial resolution due to the large probe size in LM STEM configuration,

confirming at the same time that the electric field variation is smaller than the probe size. The large camera length provides a high signal-to-noise (SNR) ratio, but the field magnitude is much lower than expected. Subsequently, a nanobeam (NB) STEM configuration was used to provide a smaller probe, with a half convergence angle of 3.2 mrad and a camera length of 2.3 m. A Quantum GIF was used for energy filtering. The unfiltered and energy-filtered diffraction patterns in the junction are shown respectively in Figs. 2(b) and (c). The corresponding maps of electric field processed by TM algorithm are shown in Figs. 2(f) and (g) and profiles are plotted in Fig. 2(i). The depletion width of the junction is again 60 nm, as the spatial resolution of the NB STEM configuration is higher. However, the magnitude of the measured electric field is still too small. Here the sharper edges provided by the energy filtering increase the SNR of the measurement, but despite a tilt of the specimen to a weakly diffracting orientation, the HOLZ lines disrupt the accurate retrieval of the shift of the transmitted beam. Finally, a beam precession system was used in the NB STEM configuration, with a tilt angle of 0.1° [6]. The precession diffraction pattern at the junction location is shown in Fig. 2(d) and the electric field retrieved by TM algorithm is shown in Fig. 2(h) and plot in Fig. 2(i). The precession system decreases the diffraction contrast. In association with TM processing it gives access to an accurate measurement of the electric field of the p - n junction.

In this presentation, as well as discussing the simple p - n junction specimen we will also present results obtained on more complex systems, such as III-V specimens where the presence of strain and interfaces between different materials present additional difficulties, or also magnetic mapping.

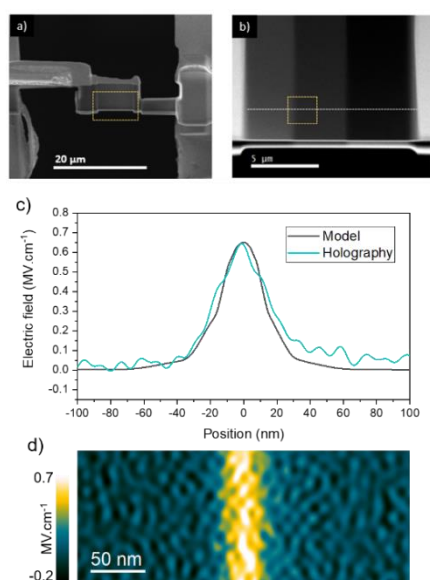


Figure 1. (a,b) STEM imaging of the p - n junction connected for *in-situ* measurement, the measurement area is circled. (c) Plots of the electric field modeled across the biased junction and measured by electron holography. (d) Displays the holography map of the electric field at the biased p - n junction.

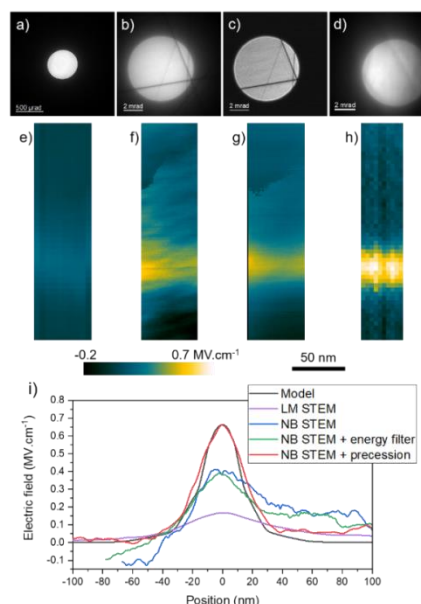


Figure 2. Diffraction patterns in the biased p - n junction measured by different pixelated STEM acquisition strategies: (a) LM, (b) NB, (c) energy filtered NB and (d) precession NB. The corresponding experimental electric field maps are shown in (e-h), respectively. (i) Plots of the electric fields measured and modeled across the junction.

References:

- [1] D Cooper, *Journal of Physics D* **49**, 474001 (2016).
- [2] C Ophus, *Microscopy and Microanalysis* **25**, 563–582 (2019).
- [3] B Haas et al., *Ultramicroscopy* **198**, 58–72 (2019).
- [4] V Boureau et al., *Journal of Physics D* **54**, 085001 (2020).
- [5] L Clark et al., *Physical Review A* **97**, 043843 (2018).
- [6] L Bruas et al., *Journal of Applied Physics* **127**, 205703 (2020).